IEEE Access
Multidisciplinary ⋮ Rapid Review ⋮ Open Access Journal

Received 6 September 2023, accepted 23 September 2023, date of publication 28 September 2023,
date of current version 5 October 2023.

Digital Object Identifier 10.1109/ACCESS.2023.3320280

RESEARCH ARTICLE

A Cost-Effective and Highly Accurate Observer for the Real-Time Estimation of the Vehicle Velocity and the Road Inclination and Bank Angles

DIMITRIOS PAPAGIANNIS, EVANGELOS TSIOUMAS, NIKOLAOS JABBOUR, AND CHRISTOS MADEMLIS, (Senior Member, IEEE)
School of Electrical and Computer Engineering, Aristotle University of Thessaloniki, 541 24 Thessaloniki, Greece

Corresponding author: Dimitrios Papagiannis (dipapagi@auth.gr)

This work was supported by the European Regional Development Fund and Greece, under the Action "Investment Plans of Innovation" of the Operational Program "Central Macedonia 2014–2020", Project KMP6-0126719.

ABSTRACT This paper proposes a low cost and low-complexity observer that can effectively and accurately estimate in real-time the longitudinal and lateral vehicle velocities, and the road inclination and bank angles. The above are needed in several systems of a vehicle, such as the battery energy management of an electric vehicle, the active suspension and other driver assistance systems. The suggested observer utilizes the neural network technique and is realized by using information provided by sensors that measure the angular velocity of the wheels, the position of the accelerator and decelerator pedals, and the angle of the steering wheel, with which the modern vehicles are usually equipped. The only additional sensors that are required are four inertial measurement units mounted on each wheel-carrier. However, they are relatively low-cost sensors and therefore, the total cost of the vehicle does not considerably increase. The training of the neural network can be easily performed in a test road. The feasibility and effectiveness of the suggested observer are verified on simulation models with the CarMaker and Matlab/Simulink programs. Several simulation results are presented to validate the satisfactory operation of the observer, which are also compared with other techniques from the literature.

INDEX TERMS Vehicle velocity, road inclination angle, road bank angle, battery management, vehicle suspension system.

I. INTRODUCTION

The vehicles are usually a field of application of new technologies for the improvement of the safety, speed, and comfort, such as active chassis control systems [1], advanced driver assistance systems [2], anti-lock braking system [3], electronic stability control [4], torque vectoring [5], and semi-active and active suspension systems [6]. For the effective operation of the above systems, the accurate knowledge of the vehicle's velocity [7], as well as the pitch and roll angles of the vehicle [8], which can be respectively estimated by the inclination and bank angles of the road, play a key role. Moreover, the accurate real-time estimation of the above variables can enhance the vehicle's performance by improving the operation of its several parts, such as the suspension system [9], [10], the steering system in autonomous electric vehicles [11], the energy management in electric vehicles [12], etc. Furthermore, it can enhance the perceptional capabilities of the driver to avoid accidents, improve driving comfort, better regulate accelerations/decelerations, avoid vehicle's overturning in sharp turns, etc. [13].

Due to the above, a growing research interest has been directed towards the development of accurate estimation methods of the vehicle velocity and the road inclination and bank angles. Regarding the vehicle velocity estimation, the methods that have been published in the technical literature can be categorized in kinematic, dynamic, and advanced-sensor based, while for the estimation of the road inclination

The associate editor coordinating the review of this manuscript and approving it for publication was Jesus Felez.

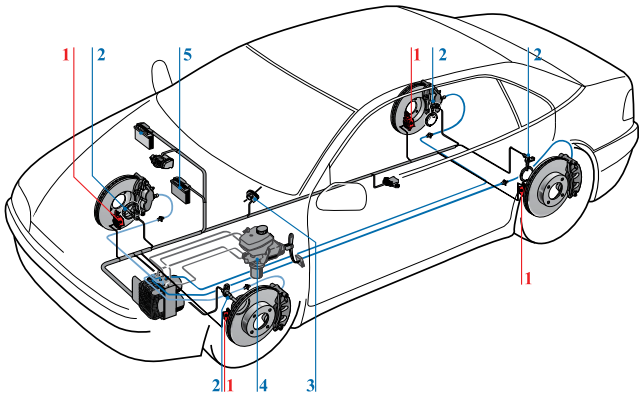

FIGURE 1. Location of the proposed IMU sensors and the other sensors and components required by the proposed technique *(1. IMU on the wheel carriers, 2. wheel speed sensors, 3. steering wheel sensor, 4. Accelerator/decelerator sensors, and 5. Controller).* Source: Adapted from [4].

and bank angles, combined kinematic and sensor-based methods have been proposed.

In the kinematic-based techniques, the velocity of the vehicle is mainly estimated by utilizing the measurements obtained by an inertial measurement unit (IMU) located on the center of gravity of the sprung mass and exploiting the kinematic differential equations of the vehicle's motion model. Specifically, in [14], the longitudinal and lateral vehicle velocities are estimated based on the measurements of the integrated six degrees of freedom sensor on the vehicle body. In [15], the vehicle longitudinal velocity is estimated based on the measurements of the rotational speed of each wheel and the longitudinal acceleration of the vehicle. The main drawback of this method is the accumulated error that is caused by the sensors' irregularities, e.g., IMU bias, gyroscopes' drift, etc. To alleviate this problem, a closed loop control system based on the Kalman filter has been proposed in [16]. Also, an extended Kalman filter and the measurements from a combined scheme of an IMU and a Global Navigation Satellite System (GNSS) have been used for the estimation of both the longitudinal and lateral velocities in [17], and the roll angle of the sprung mass and the tires' cornering stiffnesses in [18]. However, the estimations depend on the low update rate of the GNSS (typically around 1s) and its low reliability since the signal may be lost at roads between tall buildings, long road tunnels, etc. To overcome this problem, a stack bidirectional long short-term memory recurrent neural network has been proposed in [19], which estimates the GNSS sensor output value during a potential outage of the sensor, e.g. loss of the sensor signal.

In the dynamic-based methods, the vehicle velocity is estimated utilizing complex vehicle models and sensor measurements. Thus, the effectiveness of the vehicle velocity estimation depends on their accuracy and also on the potential variation of the model parameters. In particular, a dynamic model of the vehicle has been adopted in [20] to estimate the forces and torques. In addition to the vehicle model, a linear tire model has been used in [21] to increase the accuracy of the vehicle velocity estimation. However, it is mainly focused on the improvement of the accuracy of only the lateral velocity estimation. *To* effectively estimate both the lateral and longitudinal velocities, a more complex tire model has been proposed in [22] and the Dugoff's tire model has been adopted in [23].

Finally, in the advanced-sensor methods, sensors such as cameras, LiDARs, and radars are used. Specifically, an interferometric radar has been used in [24] for the vehicle velocity estimation, while a stereo vision camera for the image analysis has been utilized in [25]. An attempt to increase the accuracy of the vehicle velocity estimation by considering information of the vehicle operation has been presented in [26]. Also, a method that the longitudinal velocity of vehicle is estimated based on a long-short term memory deep neural network utilizing measurements obtained by a GNSS sensor, a radar, and data from the controller of the engine has been proposed in [27]. Although the above techniques have several advantages with respect to the accuracy of the vehicle velocity estimation, they are not affordable for general use in all vehicles since highly expensive sensors are required that considerably increase the implementation cost.

Regarding the estimation of the road inclination and bank angles, several measurement schemes have been proposed in technical literature, where usually the information of an IMU is combined with the kinematic model of the vehicle. Specifically, a finite-memory estimation method of the angles of the vehicle roll and the road bank based on measurements obtained by inertial sensors and the vehicle suspension deflection has been proposed in [28], while the kinematic model of the vehicle has been utilized in [29] and [30] for the estimation of the road bank angle.

The common characteristic of the aforementioned kinematic model-based methods is that their accuracy and effectiveness greatly depend on the accuracy of the model. For this reason, attempts for developing a combined kinematic and advanced sensor-based scheme and also considering information obtained by a GNSS sensor have been conducted. Specifically, a constrained dual Kalman filter has been proposed in [31] for the estimation of the road bank angle and the model parameters of the vehicle, utilizing the measurements from a dual antenna GNSS sensor, an IMU and a steering wheel sensor of the vehicle. A decoupling method of the road bank estimation from the roll angle of the vehicle has been proposed in [32] utilizing the extended Kalman filter architecture and measurements from the GNSS, the IMU located on the center of gravity of the vehicle and the potential suspension deflections, while only the GNSS measurements are utilized in [33] for the real time estimation of the road bank angle. However, the frequency for providing the variables estimations is low due to the low update rate of the GNSS and also, depends on the potentiality of losing its signal at roads between tall buildings, long road tunnels, etc.

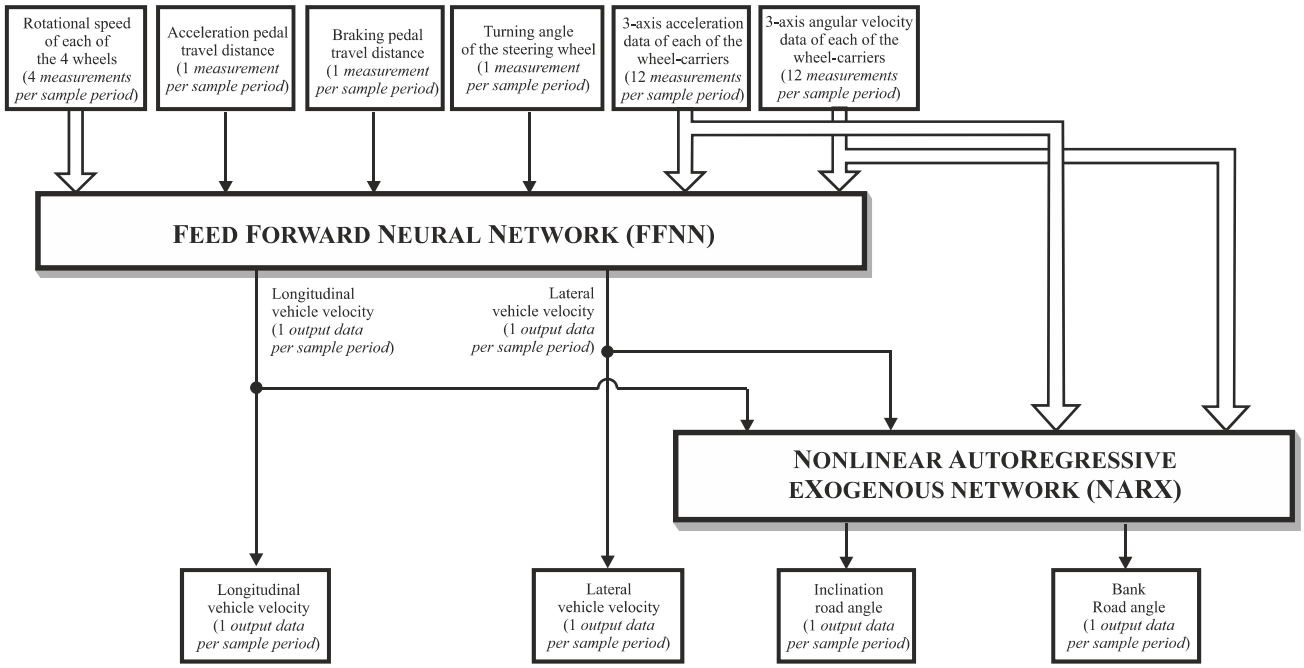

FIGURE 2. Flow chart of the proposed observer for the estimation of the longitudinal and lateral vehicle velocities and the inclination and bank road angles.

From the above reference analysis, it is concluded that the estimation of the vehicle longitudinal and lateral velocities and the road inclination and bank angles is still an open research issue. This information is crucial for the effective and proper operation of several systems of any vehicle type (conventional, electric, autonomous). Therefore, a new technique is needed that can accurately and effectively provide the above information, and it can be implemented without considerably increasing the cost of the vehicle.

Thus, aim of the paper is:

- An easily implemented and cost-effective observer which can accurately and effectively estimate, in real-time, the longitudinal and lateral velocities of a vehicle, as well as the inclination and bank angles of the road.
- The proposed observer is realized by utilizing the neural network method and therefore it does not depend on the accuracy of the vehicle model.
- The implementation of the proposed technique is based on sensors that modern vehicles are usually equipped with, and the only additional hardware is a set of four low-cost IMU sensors mounted on each wheel-carrier, as shown in Fig. 1. Therefore, unlike other techniques, a highly accurate GNSS is not required that may increase the cost of the system and the drawbacks of low update rate of the estimated variables and the potential loss of the GNSS signal at roads between tall buildings, long road tunnels, etc. that may reduce the reliability of the system are avoided.

The feasibility of the proposed observer is validated on simulation models with the CarMaker and Matlab/Simulink software. Selective simulation results are presented to demonstrate the effectiveness of the suggested technique, which are also compared with simulation results obtained by other methods from the literature that are used as benchmarks.

The rest of the paper is organized as follows. In Section II the overview of the proposed observer is explained and in Section III the training methodology is described. Simulation results are presented and discussed in Section IV and the conclusions are given in Section V.

II. OVERVIEW OF THE PROPOSED OBSERVER

The operation of the proposed observer and the measurement inputs that are used for its implementation are described in the flow chart of Fig. 2. It is composed of two stages. In the first stage, a feed forward neural network (FFNN) is used for the real-time estimation of the longitudinal and lateral velocities of a vehicle, while a nonlinear autoregressive exogenous network (NARX) is utilized at the second stage of the observer for the real-time estimation of the inclination and bank angles of a road.

The two neural networks are connected in cascade mode, since the two outputs of the FFNN of the first stage are also used as inputs to the NARX of the second stage. Since the two neural networks operate independently, there are no stability issues, as per [34] and [35]. Therefore, the convergence of the observer is always accomplished without being trapped in local extrema and it can always estimate the velocity of the vehicle and the road inclination and bank angles.

The reason behind the selection of a FFNN for the first stage of the observer is that it has low computational burden and therefore, it can quickly provide the estimation of

the vehicle velocity. This is desirable because its outputs of the longitudinal and lateral vehicle velocities are essential not only for the estimation of the road inclination and bank angles at the second stage of the observer, but also for the operation of other systems of the vehicle with high updating frequency, such as the anti-lock braking system (ABS), electronic stability program (ESP), battery management, and active suspension system [36]. Also, the FFNN can be easily implemented and hence, it does not increase the complexity of the system. Moreover, it is preferable against a recurrent neural network because each estimation of the vehicle velocity should be independent from the previous one, so as to effectively monitor dynamic states of the vehicle, such as emergency braking and fast acceleration.

For the second part of the observer, the NARX is adopted because it is more suitable for variables of nonlinear time series with unexpected fleeting transient periods [37], [38]. Moreover, it can more effectively manipulate the history of the data and damp any oscillations of the sensor measurements, such as the abnormalities of a road [6].

Note that, since the frequency of changes in the road inclination and bank angles is usually lower than that of the vehicle velocity, the operating frequency of the second part of the observer is slower than that of the first part. This is an additional reason that allows to use the estimations of the longitudinal and lateral vehicle velocities of the first part of observer as inputs to the second part of the observer.

A. OBSERVER VARIABLES

The proper selection of the observer variables and the architecture of the neural network layers play a crucial role, not only for the computational performance but also, the accuracy and the effectiveness of the observer.

For the FFNN of the first part of the observer, the rotational speed of the four wheels combined with the 3-axis angular velocities and accelerations/decelerations of the four wheel-carriers that provide information for the three-dimensional dynamic response of the unsprung mass of the vehicle, are the basic input data for the estimation of the longitudinal and lateral velocities of the vehicle. The list of the FFNN inputs is completed with the measurements of the steering wheel angle that provides information for the driving direction and the travel distances of the accelerating and braking pedals which give information for the dynamic state of the whole vehicle.

Inputs to the NARX network are the outputs of the FFNN of the first stage of the observer i.e., the longitudinal and lateral velocities, and also, the dynamic state of the unsprung mass of the vehicle which is provided by the measurement of the 3-axis angular velocity and the acceleration/deceleration of the four wheel-carriers.

It should be noted that the implementation of the proposed observer is not based on information obtained by a GNSS sensor and therefore, it is cost effective since otherwise a highly accurate GNSS sensor would be required that would increase the cost of the system. Moreover, the drawbacks of the low update rate and the potential loss of the GNSS signal at roads between tall buildings, long road tunnels, etc. are avoided. However, since some modern vehicles are usually equipped with a GNSS sensor (usually for navigation purposes), its output data could be used as complementary input to the proposed observer to increase its accuracy.

B. OBSERVER LAYERS ARCHITECTURE

Each of the FFNN and NARX topologies of the proposed observer consists of three layers, i.e., input, hidden, and output layers, so as less complex architecture and effective computational performance can be attained. The input lay-er consists of the input variables while the hidden layer comprises n neurons [39] as given by

$$n = \sqrt{\frac{N}{d \ln(N)}} \tag{1}$$

where N is the size of the training samples and d is the number of the input variables. In each of the FFNN and NARX of the two stages of the observer, every neuron of the one layer is related with the next layer through a dataset of weighting factors and biases, and by applying a tangential sigmoidal (tan-sigmoid) transfer function.

The output layer of each of the FFNN and NARX consists of only one neuron with a linear transfer function and two output variables, i.e., the longitudinal and lateral velocities from the FFNN and the road inclination and bank road angles from the NARX.

III. TRAINING OF THE OBSERVER

The training of the FFNN and NARX is realized by an optimization algorithm that provides the proper weighting factors and biases to best map inputs to outputs. The training dataset should be large enough with a wide range of variable values at both steady-state and dynamic operating conditions, so that the desired training accuracy is attained. For both FFNN and NARX, the common back-propagation technique was used for the training and the calculation of the weighting factors and the biases.

The training of the two neural networks in real life should be conducted in a test road that has several corners and ascending and descending inclinations. Also, the vehicle should run the test road several times at various speeds, with accelerations and decelerations, lateral maneuvers and in forward and rear driving, so that as many as possible operating conditions of the vehicle are emulated. Additionally, since several variables of the vehicle performance depend on the driving behavior, the vehicle should be driven during the training procedure by several drivers.

A test road with configurations as that described above has been selected because the typical test road mentioned in ISO 15037-1 [40] for the dynamic tests of a vehicle does not have the wide range of performance conditions that may be

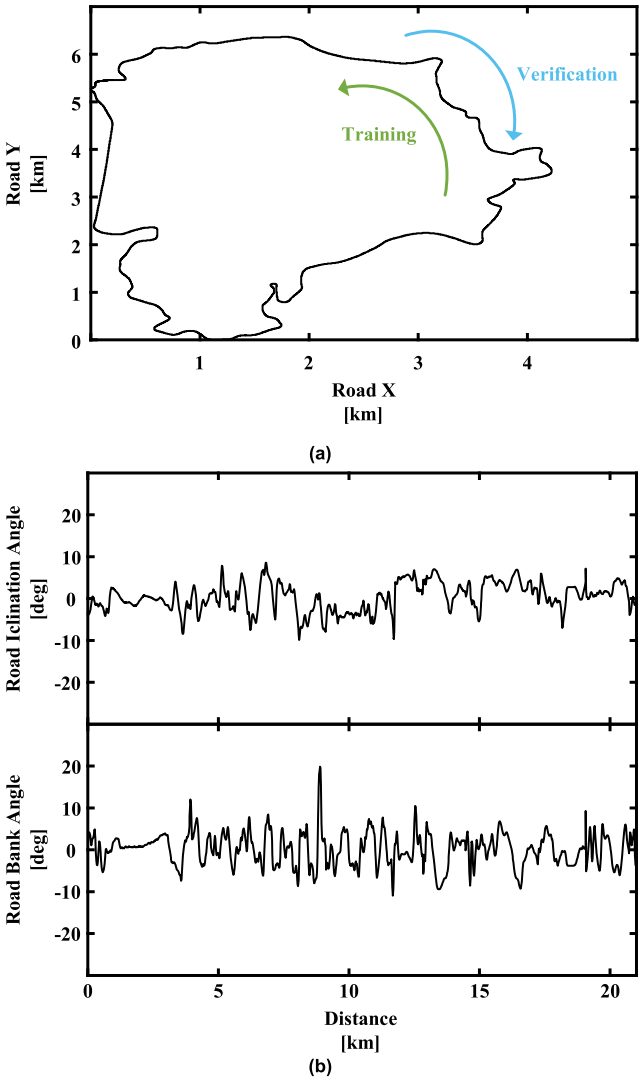

FIGURE 3. Test road: (a) 2-D overview of the course and (b) road inclination and bank angles in respect to traveled distance (training direction).

needed to satisfactorily train the two neural networks of the proposed observer. Moreover, through this, it is validated the more general applicability of the observer since the training can be performed at any test road at which as many as possible steady-state and dynamic operating condition are emulated.

The position and the velocity of the vehicle can be monitored and recorded through an indoor positioning system [41] and [42]. Thus, the FFNN and NARX of the observer are trained by utilizing the measurements of the four IMUs at the wheel carriers, the position of the accelerator and the decelerator pedals, the angle of the steering wheel measured by the respective sensors, and also considering the morphology of the test road.

In this paper, in order to examine the effectiveness of the training process, the model of a typical Class D vehicle is used [43] and its technical specifications are reported in

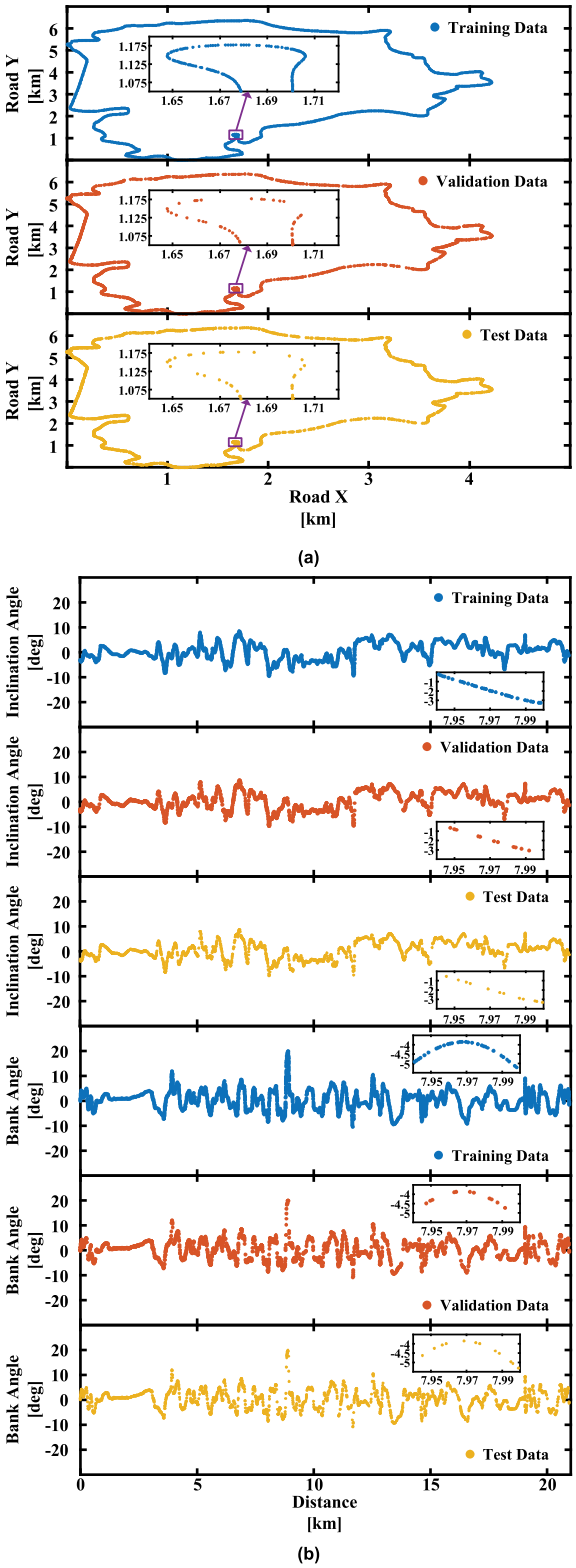

FIGURE 4. Measurement sample points of the test road that have been used as training, validation, and test data to verify the effectiveness of the training of the observer: (a) 2-D overview and (b) rod inclination and bank angles.

Table 1. The simulations have been conducted in a cooperating scheme of the programs MATLAB/Simulink and IPG

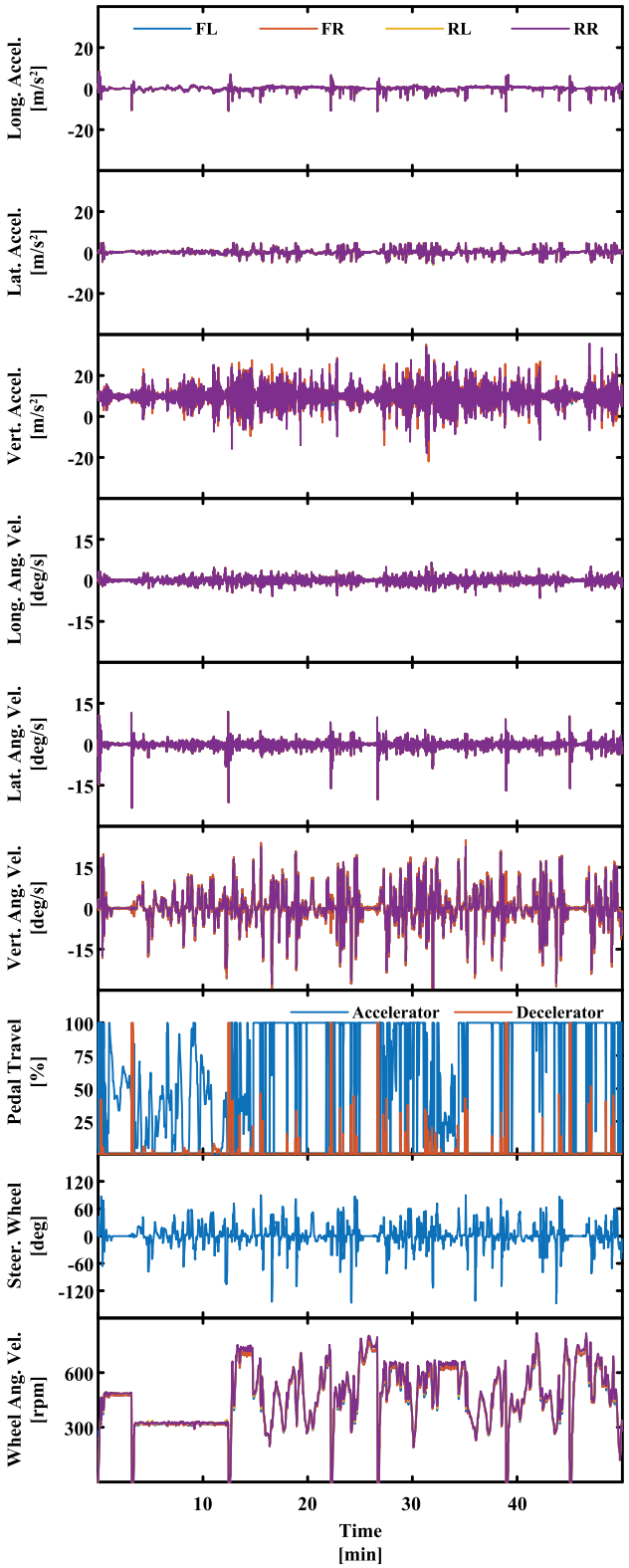

FIGURE 5. Recorded data of the input variables by the one driver of the vehicle that have been used for the training of the observer. (FL: Front Left, RL: Front Right, RL: Rear Left, RR: Rear Right Wheel or Wheel Carrier).

CarMaker. A test road course, such as that illustrated in Fig. 3, has been considered for the simulation analysis of the

TABLE 1. Class D Vehicle Technical Specifications.

Sprung Mass [kg]	1670
Front Unsprung Mass [kg]	47.5
Rear Unsprung Mass [kg]	57
Wheelbase [m]	2.8
Front Track Width [m]	1.574
Rear Track Width [m]	1.574
Wheelbase [m]	2.8
Weight Distribution [%]	50
Front Axle Tire Radius [m]	0.33
Rear Axle Tire Radius [m]	0.33

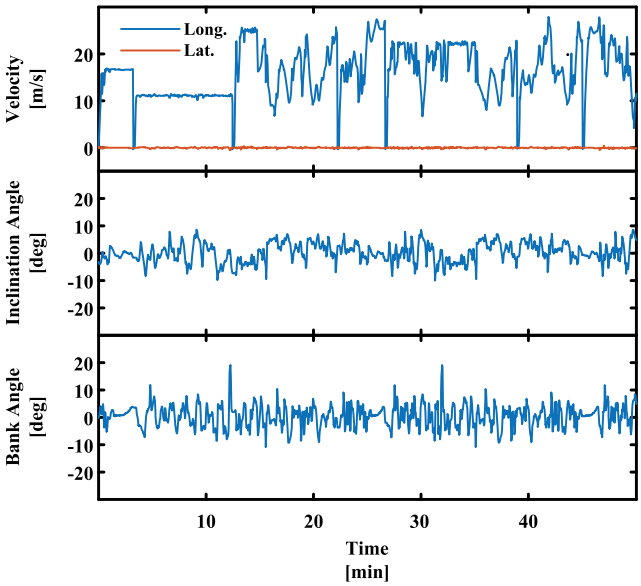

FIGURE 6. Vehicle velocity and road inclination and bank angles that have been used as target values during the training of the observer.

observer training procedure. Specifically, the road course in two dimensions is illustrated in Fig. 3(a), while the inclination and bank angles of the test road in respect to the traveled distance of the vehicle towards the training direction are presented in Fig. 3(b). The measurement sample points of the test road that have been used as training, validation, and test data to verify the effectiveness of the training of the observer are illustrated in two dimensions of the road course in Fig. 4(a) and with respect to the road inclination and bank angles in Fig. 4(b).

The data of the driving performance of the vehicle, as well as the behavior of the driver, that were used for the training of the observer are presented in Figs. 5 and 6. Specifically, the input training values of the observer, which are the longitudinal, lateral, and vertical accelerations and angular velocities of the WCs, as well as the pedal movement and the steering wheel turning angle, and finally the angular velocity of the wheels are illustrated in Fig. 5. Also, the velocity of the vehicle and the inclination and bank angles of the road, which

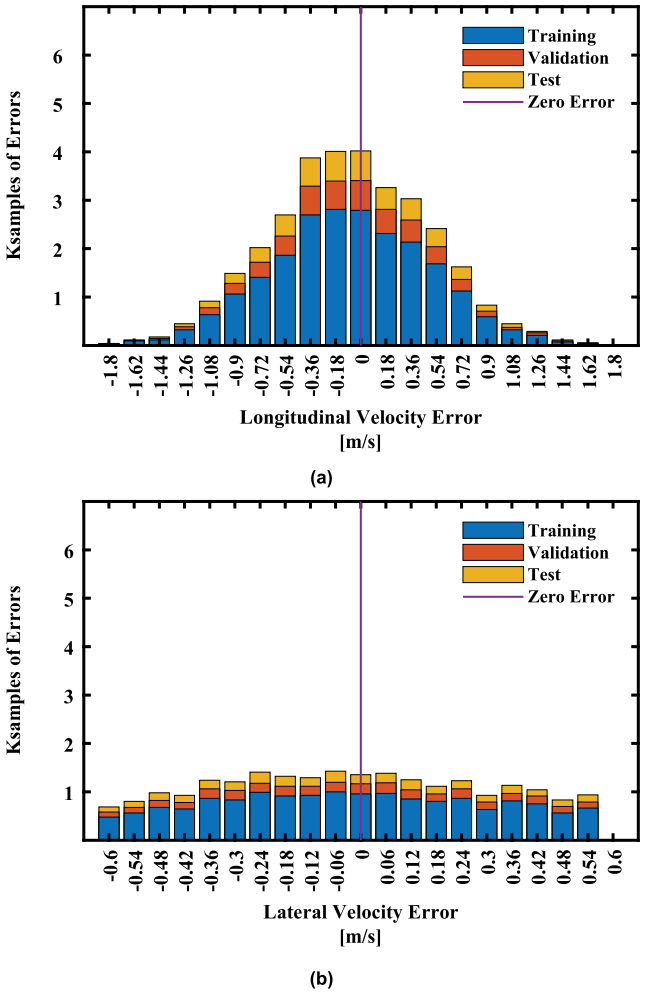

FIGURE 7. Error histograms of the training process of the FFNN, for: (a) the longitudinal velocity and (b) the lateral velocity.

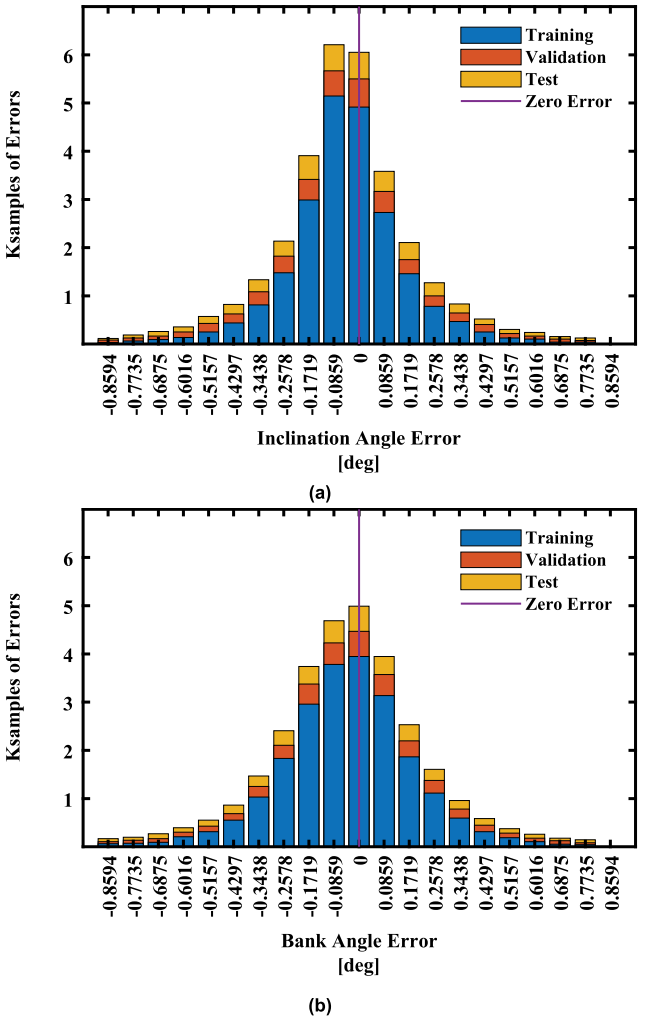

FIGURE 8. Error histograms of the training process of the NARX, for: (a) the inclination angle and (b) the bank angle of the road.

are used as the training target values of the observer during the 50 min driving at the training test road are shown in Fig. 6. In Figs. 5 and 6, the input data and target values correspond to one driver of the vehicle, while several different drivers have been used to develop the whole data set of the training of the observer.

The effectiveness of the observer training procedure is validated in Figs. 7 and 8. Specifically, the error histograms of the FFNN training for the longitudinal and lateral velocities are presented in Figs. 7(a) and (b), respectively, and the error histograms of the NARX training for the road inclination and bank angles are given in Figs. 8(a) and (b), respectively. As can be seen, in both FFNN and NARX, the error of the observer outputs during the training with respect to the actual values are within an acceptable range and only a relatively small number of error samples is out of the acceptable range.

Specifically, in Fig. 7(a), for the 22ksamples of the training, longitudinal velocity error out of the acceptable range of ± 1.08m/s occurs in less than 2ksamples, while in the 5ksamples of the validation procedure and the 5ksamples of the test procedure, error samples out of the acceptable range of ± 1.08m/s are less than 500 and 450, respectively. For the lateral velocity, Fig. 7(b), error samples out of the acceptable range of ± 0.36m/s are observed in 4ksamples from the 22ksamples of the training and error samples in the validation and test procedures out of the acceptable range of ± 0.36m/s are less than 1ksamples and 0.8ksamples, respectively from the 5ksamples of each procedure. Similar acceptable error ranges are observed for the road inclination and bank angles, as can be seen in Figs. 8(a) and (b), respectively.

IV. SIMULATION RESULTS

To verify the effectiveness of the proposed technique, a simulation study is performed, and the estimation outcomes of the proposed observer are compared with published techniques in the literature, which are used as benchmark. For the space economy in the paper, the same road course as that used for the training of the observer (Fig. 3) has been considered for the simulation analysis and thus, it is not needed further description of the test road. However, to differentiate the

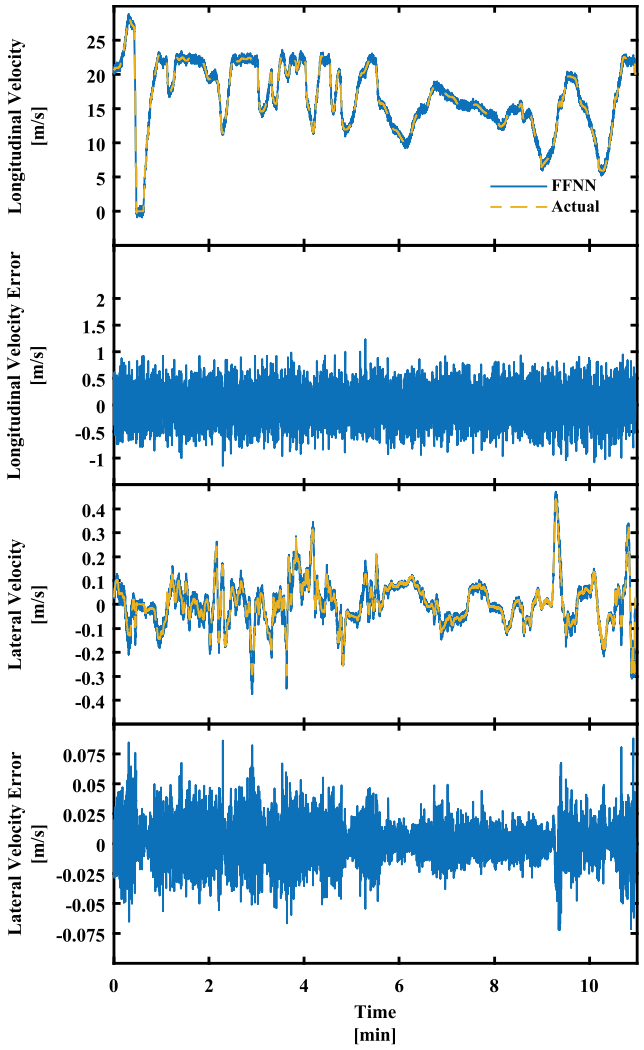

FIGURE 9. Comparison between the estimated longitudinal and lateral vehicle velocities by the FFNN of the first part of the observer with the actual values.

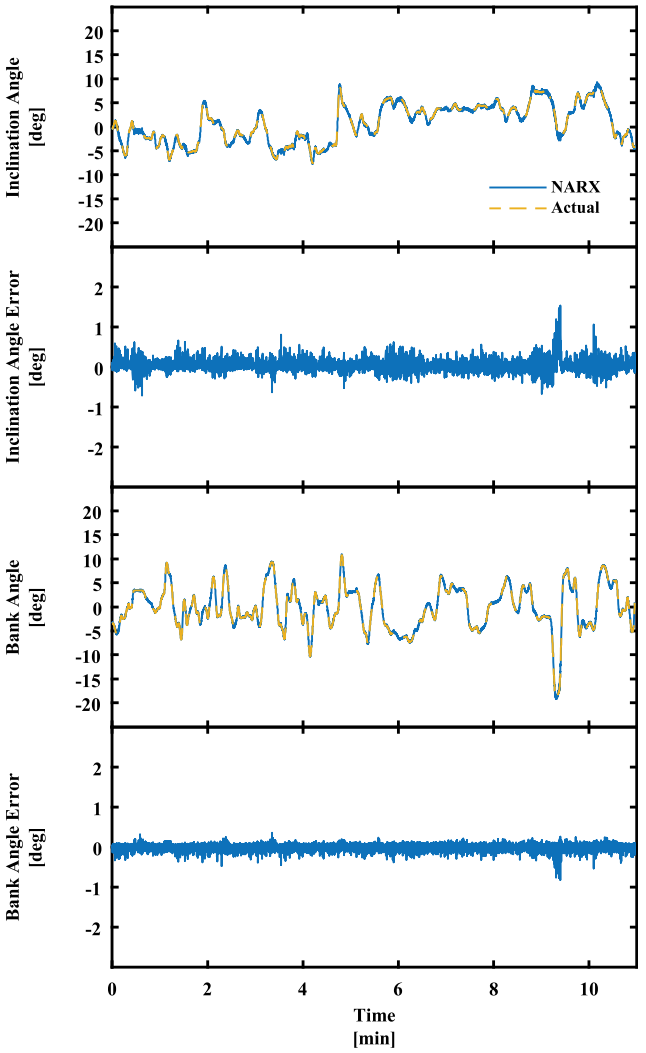

FIGURE 10. Comparison between the estimated inclination and bank road angles by the NARX of the second part of the observer with the actual values.

simulation study from the training results, the opposite driving direction is followed and also, different driving behavior than that used for the training of the observer is considered in velocity variations and accelerations/decelerations. Finally, to come closer to the real sensors performance whose characteristics are taken from typical sensor datasheets [44], [45], [46], [47], white noise has been added on the sensors' measurements.

The evaluation of the accuracy of the estimated variables is conducted on the basis of typical neural network metrics. Specifically, the maximum error range (MER):

$$MER = \left[\min(A_i^{act} - A_i^{est}) \ \max(A_i^{act} - A_i^{est}) \right] \quad (2)$$

the mean absolute error (MAE):

$$MAE = \frac{1}{M} \sum_{i=1}^{M} |A_i^{act} - A_i^{est}| \quad (3)$$

and the root mean square error (RMSE):

$$RMSE = \sqrt{\frac{1}{M} \sum_{i=1}^{M} (A_i^{act} - A_i^{est})^2} \quad (4)$$

in a round of the test road are used, where A_i^{act} and A_i^{est} are the actual and the estimated values of the $i-$th sample of a variable A, respectively, and M is the total number of samples of the estimation dataset. The outputs of the comparisons for the MER, MAE and RMSE are summarized in Tables 2, 3 and 4, respectively.

A. PERFORMANCE OF THE PROPOSED OBSERVER

In Figs. 9 and 10, the estimations of the proposed observer are compared with the respective actual values. Specifically, the longitudinal and lateral velocities estimated by the FFNN are compared with the respective actual values in Fig. 9, and the road inclination and bank angles estimated by the

TABLE 2. Comparison of the MER of the estimated variables by the proposed observer against [21] and [32].

Estimated vehicle velocities [m/s]	FFNN	Ref [21]	Ref [32]
Longitudinal Velocity	-1.13…1.13	-0.66…2.67	-0.05…0.08
Lateral Velocity	-0.075…0.075	-0.085…0.085	-0.085…0.069
Estimated road angles [deg]	**NARX**	**Ref [32]**	
Inclination Angle	-0.7…1.5	-2.9…1.8	
Bank Angle	-0.8…0.35	-1.76…2.34	

TABLE 3. Comparison of the MAE of the Estimated Variables by the Proposed Observer Against [21] and [32].

Estimated vehicle velocities [m/s]	FFNN	Ref [21]	Ref [32]
Longitudinal Velocity	0.25	0.65	0.018
Lateral Velocity	0.01	0.016	0.009
Estimated road angles [deg]	**NARX**	**Ref [32]**	
Inclination Angle	0.1	0.19	
Bank Angle	0.06	0.46	

TABLE 4. Comparison of the RMSE of the estimated variables by the proposed observer against [21] and [32].

Estimated vehicle velocities [m/s]	FFNN	Ref [21]	Ref [32]
Longitudinal Velocity	0.32	0.73	0.023
Lateral Velocity	0.016	0.02	0.02
Estimated road angles [deg]	**NARX**	**Ref [32]**	
Inclination Angle	0.015	0.25	
Bank Angle	0.09	0.60	

NARX are compared with the respective actual values in Fig. 10.

As can be seen, the estimated values of all variables from both parts of the observer match the respective actual values with satisfactorily accuracy. The MER of the longitudinal and lateral velocities is ±1.13m/s and ±0.075m/s, respectively, the MAE is 0.25m/s and 0.01m/s, respectively, and the RMSE is 0.32m/s and 0.016m/s, respectively (Fig. 9). The MER of the road inclination and bank road angles is from -0.7 to 1.5deg, and -0.8 to 0.35deg, respectively, the MAE is 0.1deg and 0.06deg, respectively, and the RMSE is 0.015deg and 0.09deg, respectively (Fig. 10). It should be noted that the above errors are mainly owed to the white noise that has been added on purpose in the sensors' measurements to simulate the real conditions more accurately. Thus, if higher accuracy in the estimations by the proposed observer is required, higher accuracy sensors should be used and also, the measuring conditions should be improved (e.g., proper filtering in the measurements, immunity against interferences, etc.).

B. COMPARISON WITH OTHER TECHNIQUES

To highlight the advantages of the proposed estimation observer, not only with respect to the accuracy but also on the effectiveness and practicality, the results of Figs. 9 and 10 are compared with two other techniques from the literature.

1) LONGITUDINAL AND LATERAL VELOCITIES

In Fig. 11, the estimations of the longitudinal and lateral velocities, which are the first part of the observer (FFNN), are compared with the techniques of [21] and [32]. In order to make the comparisons easier, the performance of the output of the observer (FFNN) of Fig. 9 is also repeated in Fig. 11.

In [21], that is usually used in odometry, the longitudinal and lateral velocities of the vehicle are estimated through a Kalman filter by combining information obtained by an IMU located at the center of gravity of the vehicle frame, the angular speed of the wheels, as well as the steering angle, the kinematic model of the vehicle, and the dynamic model of the tires. In [32], the longitudinal and lateral velocities of the vehicle are estimated based on the data obtained by the combination of an IMU and a highly accurate and consequently costly GNSS sensor.

As you can see, the MER of the longitudinal velocity estimated by [21] is from −0.66 to +2.67m/s, the MAE is 0.65m/s and the RMSE is 0.73m/s, respectively, and also there is a mean deviation error of almost 0.65m/s with respect to the actual values. Contrarily, the respective MER with the FFNN of the proposed observer is confined to ±1.13m/s with MAE 0.25m/s and RMSE 0.32m/s. The difference of the estimation error in the lateral velocity between [21] and the proposed observer is lower. Specifically, the MER of [21] is ±0.085m/s with MAE 0.016m/s and RMSE 0.02m/s, while the respective MER of the proposed observer, as aforementioned, is ±0.075m/s, the MAE is 0.01m/ and the RMSE is 0.016m/s, respectively.

The higher estimation accuracy of both longitudinal and lateral velocities with the proposed observer is owed to the fact that, the driving conditions and the dynamic performance of the tires are considered by the FFNN, through the utilization of the IMUs located on the wheel carriers, whereas they are ignored in [21] and the effective radius of each tire of the vehicle is considered constant. On the other hand, since the estimation of the lateral accuracy is not considerably affected by the variation of each tire's radius, there is no high difference between the estimations of the proposed observer and the technique of [21].

The estimation of the longitudinal velocity with the technique of [32] has considerably lower error compared to the actual values (MER from −0.05 to 0.08m/s, MAE 0.018m/s

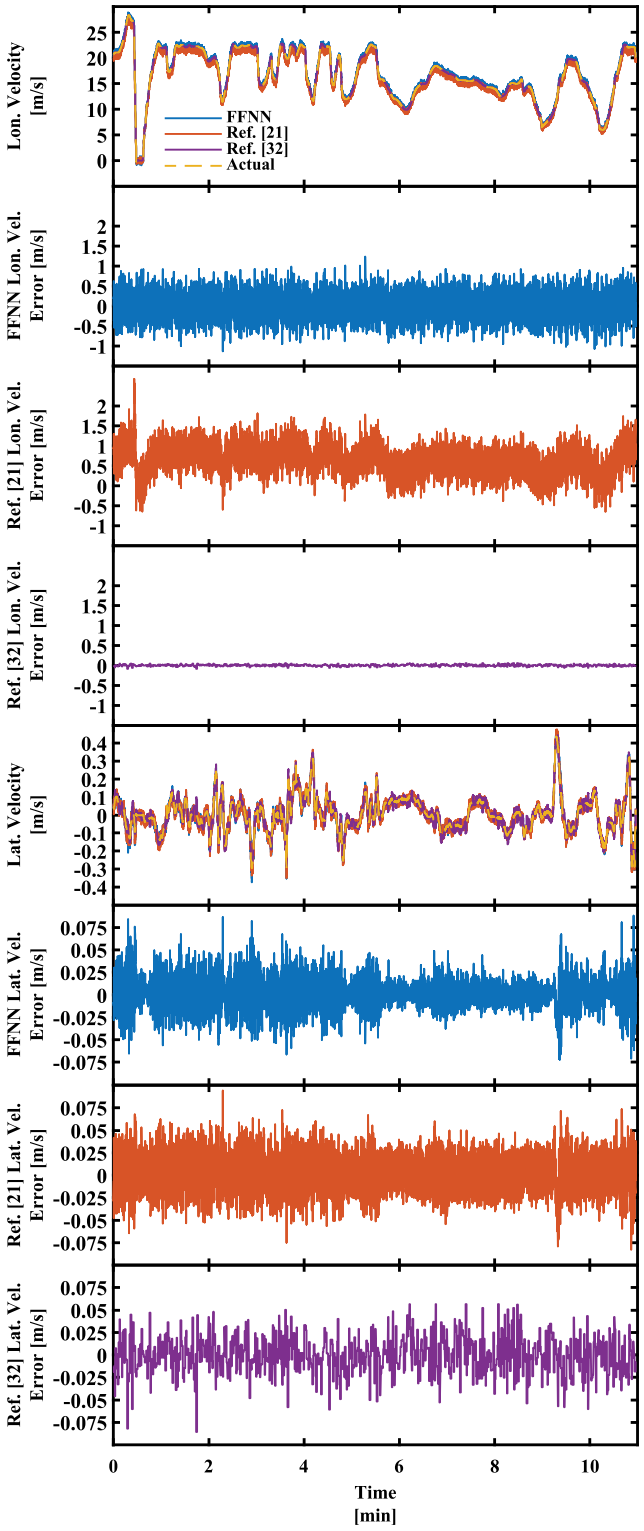

FIGURE 11. Comparison between the estimated longitudinal and lateral velocities provided by the FFNN of the proposed observer with those obtained by the techniques [21] and [32].

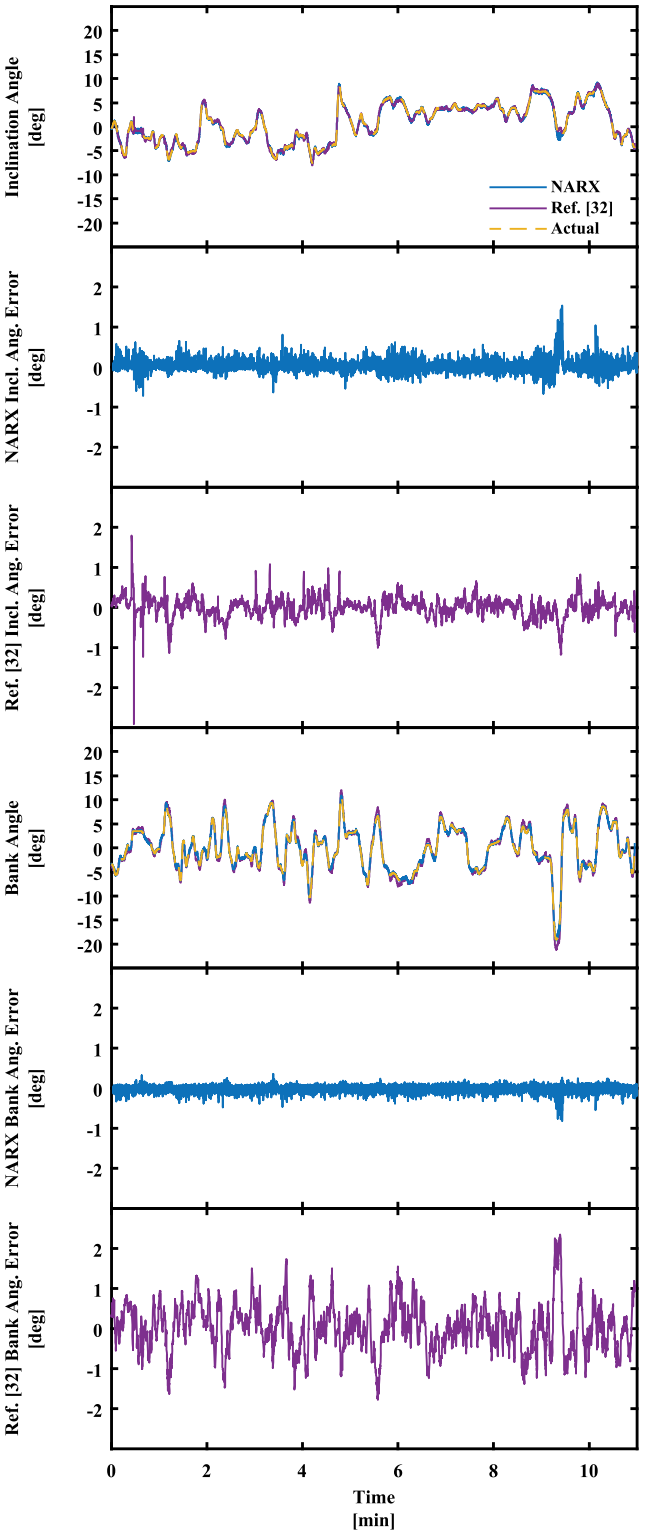

FIGURE 12. Comparison between the estimated road inclination and bank angles provided by the NARX of the proposed observer with those obtained by the technique [32].

and RMSE 0.023m/s by [32], against MER ±1.13m/s, MAE 0.25m/s and RMSE 0.32m/s of the proposed observer). At this aspect, [32] might outweigh the proposed observer; however, a highly accurate GNSS sensor is required that increases the cost of the system and also has the drawbacks of low update rate and potential loss of its signal at

roads between tall buildings, long road tunnels, etc., which decreases the effectiveness of the system. Considering the above disadvantages of [32], the proposed observer may be more preferable for broad application, since it is cost effective and attains satisfactory accuracy with a relatively high update rate of the estimated variables.

2) ROAD INCLINATION AND BANK ANGLES

The estimations of the road inclination and bank angles from the second part of the proposed observer are compared with that obtained by using the technique of [32]. Note that in [32], the pitch and roll angles of both the vehicle and the road are initially estimated and then the inclination and bank angles of the road are extracted from the sprung mass inclination and bank angles, respectively. Thus, the opposite way in the calculations is followed against that of the proposed observer where the road inclination and bank angles are initial estimated and then the pitch and roll angles of the sprung mass.

In Fig. 12, the estimated road inclination and bank angles obtained by the NARX are compared with those estimated by the technique of [32]. In order to make the comparisons easier, the performance of the output of the observer (NARX) of Fig. 10 is also repeated in Fig. 12. As can be seen, in both estimated variables, the accuracy of the proposed observer is higher than that of [32]. Specifically, the MER of the estimated road inclination angle with [32] is from -2.9 to $+1.8$deg, the MAE is 0.19deg and the RMSE is 0.25deg, whereas they are -0.7 to 1.5deg, 0.1deg and 0.015deg, respectively, with the proposed observer. For the estimated road bank angle, the MER is from -1.76 to 2.34deg, the MAE is 0.46deg and the RMSE is 0.6deg with [32], whereas they are -0.8 to 0.35deg, 0.06deg and 0.09deg, respectively, with the proposed observer. The higher error in both the estimated road inclination and bank angles by the technique of [32] may be attributed to the time delay that is owed to the Kalman filter.

V. CONCLUSION

This paper proposes an observer for the effective and accurate real time estimation of the longitudinal and lateral vehicle velocities and the road inclination and bank angles. The proposed observer is composed of two stages, where in each stage a properly trained neural network is used. Specifically, a feed forward neural network (FFNN) is used for the real-time estimation of the longitudinal and lateral velocities of a vehicle, while a nonlinear autoregressive exogenous network (NARX) is utilized at the second stage of the observer for the real-time estimation of the road inclination and bank angles.

For the implementation of the proposed observer, information obtained by sensors that measure the angular velocity of the wheels, the position of the accelerator and decelerator pedals, and the angle of the steering wheel are utilized, that the modern vehicles are usually equipped. The only additional hardware that is required is a set of four inertial measurement units (IMUs) mounted on the four wheel-carrier. However, since they are relatively low-cost sensors, the total cost of the vehicle has not been considerably increased. The training of the neural network can be easily performed in a test road.

The CarMaker and Matlab/Simulink programs have been used for the simulation analysis to validate the feasibility and the effectiveness of the suggested observer and selective simulation results have been presented. Moreover, the simulation results of the proposed observer are compared with that of other techniques from the literature and it was validated that satisfactory accuracy is attained with reduced hardware requirements and without being based on a model or utilizing a GNSS.

REFERENCES

[1] R. Rajamani, *Vehicle Dynamics and Control*. Boston, MA, USA: Springer, 2012.

[2] L. Li and F.-Y. Wang, *Advanced Motion Control and Sensing for Intelligent Vehicles*. Boston, MA, USA: Springer, 2007.

[3] S. M. Saravesi and M. Tanelli, *Active Braking Control Systems Design for Vehicles*. London, U.K.: Springer, 2010.

[4] K. Reif, *Brakes, Brake Control and Drivers Assistance System Function, Regulation and Components*. Cham, Switzerland: Springer, 2014.

[5] C. Chatzikomis, A. Sorniotti, P. Gruber, M. Zanchetta, D. Willans, and B. Balcombe, "Comparison of path tracking and torque-vectoring controllers for autonomous electric vehicles," *IEEE Trans. Intell. Vehicles*, vol. 3, no. 4, pp. 559–570, Dec. 2018.

[6] D. Papagiannis, E. Tsioumas, M. Koseoglou, N. Jabbour, and C. Mademlis, "Enhancing the braking performance of a vehicle through the proper control of the active suspension system," *IEEE Access*, vol. 9, pp. 155936–155948, 2021.

[7] H. Ahmed and M. Tahir, "Accurate attitude estimation of a moving land vehicle using low-cost MEMS IMU sensors," *IEEE Trans. Intell. Transp. Syst.*, vol. 18, no. 7, pp. 1723–1739, Jul. 2017.

[8] L. Xu and H. Eric Tseng, "Robust model-based fault detection for a roll stability control system," *IEEE Trans. Control Syst. Technol.*, vol. 15, no. 3, pp. 519–528, May 2007.

[9] X. Jin, J. Wang, X. He, Z. Yan, L. Xu, C. Wei, and G. Yin, "Improving vibration performance of electric vehicles based on in-wheel motor-active suspension system via robust finite frequency control," *IEEE Trans. Intell. Transp. Syst.*, vol. 24, no. 2, pp. 1631–1643, Feb. 2023, doi: 10.1109/TITS.2022.3224609.

[10] X. Jin, J. Wang, Z. Yan, L. Xu, G. Yin, and N. Chen, "Robust vibration control for active suspension system of in-wheel-motor-driven electric vehicle via μ-synthesis methodology," *J. Dyn. Syst., Meas., Control*, vol. 144, no. 5, May 2022, doi: 10.1115/1.4053661.

[11] X. Jin, Q. Wang, Z. Yan, and H. Yang, "Nonlinear robust control of trajectory-following for autonomous ground electric vehicles with active front steering system," *AIMS Math.*, vol. 8, no. 5, pp. 11151–11179, 2023, doi: 10.3934/math.2023565.

[12] S. Milosšević and J. Milić, "Speed perception in road curves," *J. Saf. Res.*, vol. 21, no. 1, pp. 19–23, Mar. 1990, doi: 10.1016/0022-4375(90)90044-c.

[13] S. Milosevic and J. Milic, "Guiding drivers towards safer driving speed: Exploiting visual dominance in speed adaptation," *J. Saf. Res.*, vol. 90, pp. 405–438, 2022, doi: 10.1016/0022-4375(90)90044-C.

[14] W. Klier, A. Reim, and D. Stapel, "Robust estimation of vehicle sideslip angle—An approach W/O vehicle and tire models," in *Proc. SAE World Congr. Exhib.*, Detroit, MI, USA, Apr. 2008, pp. 1–7.

[15] M. Tanelli, S. M. Savaresi, and C. Cantoni, "Longitudinal vehicle speed estimation for traction and braking control systems," in *Proc. IEEE IEEE Conf. Comput. Aided Control Syst. Design Int. Conf. Control Appl. Int. Symp. Intell. Control*, Oct. 2006, pp. 2790–2795.

[16] X. Ding, Z. Wang, L. Zhang, and C. Wang, "Longitudinal vehicle speed estimation for four-wheel-independently-actuated electric vehicles based on multi-sensor fusion," *IEEE Trans. Veh. Technol.*, vol. 69, no. 11, pp. 12797–12806, Nov. 2020.

[17] L. Xiong, X. Xia, Y. Lu, W. Liu, L. Gao, S. Song, and Z. Yu, "IMU-based automated vehicle body sideslip angle and attitude estimation aided by GNSS using parallel adaptive Kalman filters," *IEEE Trans. Veh. Technol.*, vol. 69, no. 10, pp. 10668–10680, Oct. 2020.
[18] D. M. Bevly, J. Ryu, and J. Christian Gerdes, "Integrating INS sensors with GPS measurements for continuous estimation of vehicle sideslip, roll, and tire cornering stiffness," *IEEE Trans. Intell. Transp. Syst.*, vol. 7, no. 4, pp. 483–493, Dec. 2006.
[19] B. Zhang, W. Zhao, S. Zou, H. Zhang, and Z. Luan, "A reliable vehicle lateral velocity estimation methodology based on SBI-LSTM during GPS-outage," *IEEE Sensors J.*, vol. 21, no. 14, pp. 15485–15495, Jul. 2021, doi: 10.1109/JSEN.2020.3022056.
[20] A. Katriniok and D. Abel, "Adaptive EKF-based vehicle state estimation with online assessment of local observability," *IEEE Trans. Control Syst. Technol.*, vol. 24, no. 4, pp. 1368–1381, Jul. 2016.
[21] A. Rezaeian, A. Khajepour, W. Melek, S. Chen, and N. Moshchuk, "Simultaneous vehicle real-time longitudinal and lateral velocity estimation," *IEEE Trans. Veh. Technol.*, vol. 66, no. 3, pp. 1950–1962, Mar. 2017, doi: 10.1109/TVT.2016.2580700.
[22] L.-H. Zhao, Z.-Y. Liu, and H. Chen, "Design of a nonlinear observer for vehicle velocity estimation and experiments," *IEEE Trans. Control Syst. Technol.*, vol. 19, no. 3, pp. 664–672, May 2011.
[23] H. Dugoff, P. S. Fancher, and L. Segel, "An analysis of tire traction properties and their influence on vehicle dynamic performance," SAE Tech. Paper 700377, 1970.
[24] E. Klinefelter and J. A. Nanzer, "Automotive velocity sensing using millimeter-wave interferometric radar," *IEEE Trans. Microw. Theory Techn.*, vol. 69, no. 1, pp. 1096–1104, Jan. 2021.
[25] R. G. Lins, S. N. Givigi, and P. R. G. Kurka, "Velocity estimation for autonomous vehicles based on image analysis," *IEEE Trans. Instrum. Meas.*, vol. 65, no. 1, pp. 96–103, Jan. 2016.
[26] Y. Wang, Z. Zhou, C. Wei, Y. Liu, and C. Yin, "Host–target vehicle model-based lateral state estimation for preceding target vehicles considering measurement delay," *IEEE Trans. Ind. Informat.*, vol. 14, no. 9, pp. 4190–4199, Sep. 2018.
[27] T. D. Gaikwad, "Vehicle velocity prediction using artificial neural network and effect of real world signals on prediction window," SAE Tech. Paper 2020-01-0729, 2020, doi: 10.4271/2020-01-0729.
[28] H. B. Jeong, C. K. Ahn, S. H. You, and K. M. Sohn, "Finite-memory estimation for vehicle roll and road bank angles," *IEEE Trans. Ind. Electron.*, vol. 66, no. 7, pp. 5423–5432, Jul. 2019, doi: 10.1109/TIE.2018.2868295.
[29] Y.-W. Liao and F. Borrelli, "An adaptive approach to real-time estimation of vehicle sideslip, road bank angles, and sensor bias," *IEEE Trans. Veh. Technol.*, vol. 68, no. 8, pp. 7443–7454, Aug. 2019, doi: 10.1109/TVT.2019.2919129.
[30] E. Hashemi, A. Khajepour, N. Moshchuk, and S.-K. Chen, "Real-time road bank estimation with disturbance observers for vehicle control systems," *IEEE Trans. Control Syst. Technol.*, vol. 30, no. 1, pp. 443–450, Jan. 2022, doi: 10.1109/TCST.2021.3062384.
[31] B. L. Boada, D. Garcia-Pozuelo, M. J. L. Boada, and V. Diaz, "A constrained dual Kalman filter based on pdf truncation for estimation of vehicle parameters and road bank angle: Analysis and experimental validation," *IEEE Trans. Intell. Transp. Syst.*, vol. 18, no. 4, pp. 1006–1016, Apr. 2017, doi: 10.1109/TITS.2016.2594217.
[32] L. Brown and D. Bevly, "Roll and bank estimation using GPS/INS and suspension deflections," *Electronics*, vol. 4, no. 1, pp. 118–149, Jan. 2015.
[33] J.-O. Hahn, R. Rajamani, S.-H. You, and K. I. Lee, "Real-time identification of road-bank angle using differential GPS," *IEEE Trans. Control Syst. Technol.*, vol. 12, no. 4, pp. 589–599, Jul. 2004, doi: 10.1109/TCST.2004.825131.
[34] M. Forti, P. Nistri, and D. Papini, "Global exponential stability and global convergence in finite time of delayed neural networks with infinite gain," *IEEE Trans. Neural Netw.*, vol. 16, no. 6, pp. 1449–1463, Nov. 2005, doi: 10.1109/TNN.2005.852862.
[35] Z. Li, W. Wu, and Y. Tian, "Convergence of an online gradient method for feedforward neural networks with stochastic inputs," *J. Comput. Appl. Math.*, vol. 163, no. 1, pp. 165–176, Feb. 2004, doi: 10.1016/j.cam.2003.08.062.
[36] *2018/858/EU, Directive on the Approval and Market Surveillance of Motor Vehicles and Their Trailers, and of Systems, Components and Separate Technical Units Intended for Such Vehicles*. Accessed: Jun. 14, 2018. [Online]. Available: https://eur-lex.europa.eu/legal-content/EN/TXT/PDF/?uri=CELEX:32018R0858
[37] P. M. Norgaard, O. Ravn, N. K. Poulsen, and L. K. Hansen, *Neural Networks for Modelling and Control of Dynamic Systems—A Practitioner's Handbook*. London, U.K.: Springer, 2000.
[38] M. S. H. Lipu, A. Hussain, M. H. M. Saad, A. Ayob, and M. A. Hannan, "Improved recurrent NARX neural network model for state of charge estimation of lithium-ion battery using PSO algorithm," in *Proc. IEEE Symp. Comput. Appl. Ind. Electron. (ISCAIE)*, Apr. 2018, pp. 354–359, doi: 10.1109/ISCAIE.2018.8405498.
[39] J. Ponocko and J. V. Milanovic, "Forecasting demand flexibility of aggregated residential load using smart meter data," *IEEE Trans. Power Syst.*, vol. 33, no. 5, pp. 5446–5455, Sep. 2018.
[40] *Road Vehicles—Vehicle Dynamics Test Methods—Part 1: General Conditions for Passenger Cars*, Standard ISO 15037-1:2019, Geneva, Switzerland, 2019.
[41] *VBOX Automotive*. Accessed: May 15, 2023. [Online]. Available: https://www.vboxautomotive.co.uk/index.php/en/products/indoor-positioning/vips
[42] *VBOX Automotive*. Accessed: May 15, 2023. [Online]. Available: https://www.vboxautomotive.co.uk/index.php/en/products/data-loggers/vbox-3i-adas
[43] *Mechanical Vibration-Road Surface Profiles-Reporting of Measured Data*, Standard ISO 8608:2016, Geneva, Switzerland, 2016.
[44] R. Bosch GmbH. (2023). *Bosch Motorsport*. [Online]. Available: https://www.bosch-motorsport.com/content/downloads/Raceparts/en-GB/54425995191962507.html
[45] R. Bosch GmbH. (2023). *Bosch Motorsport*. [Online]. Available: https://www.bosch-motorsport.com/content/downloads/Raceparts/en-GB/51639307319190667.html#/Tabs=51650955/
[46] R. Bosch GmbH. (2023). *Bosch Motorspor*. [Online]. Available: https://www.bosch-motorsport.com/content/downloads/Raceparts/en-GB/53422859208177803.html
[47] R. Bosch GmbH. (2023). *Bosch Motorsport*. [Online]. Available: https://www.bosch-motorsport.com/content/downloads/Raceparts/en-GB/200065291246554635.html#/Tabs=9007199454820875/

DIMITRIOS PAPAGIANNIS was born in Kranea, Elassonas, Greece, in December 1990. He received the Dipl.-Eng. degree from the School of Electrical and Computer Engineering, Aristotle University of Thessaloniki, Greece, in 2015, where he is currently pursuing the Ph.D. degree in the area of optimization of vehicles' active suspension systems.

His research interests include the performance improvement of active suspension systems in vehicles, vehicle dynamics, electric motor drives, power electronics, and embedded systems design.

EVANGELOS TSIOUMAS was born in Kompotades, Fthiotidas, Greece, in June 1988. He received the Dipl.-Eng. and Ph.D. degrees in electrical and computer engineering from the Aristotle University of Thessaloniki, Greece, in 2013 and 2022, respectively.

His research interests include energy management in power systems, control optimization in microgrids, large-scale electric energy storage systems, and embedded systems design.

NIKOLAOS JABBOUR was born in Thessaloniki, Greece, in December 1988. He received the Dipl.-Eng. and Ph.D. degrees in electrical and computer engineering from the Aristotle University of Thessaloniki, Greece, in 2012 and 2018, respectively.

Since 2018, he has been with the Electrical Machines Laboratory, School of Electrical and Computer Engineering, Aristotle University of Thessaloniki, as a Postdoctoral Researcher. His research interests include control optimization, electrical machines and drives, power electronics, embedded systems, renewable energy systems, smart grids, and energy management in nearly zero energy buildings.

CHRISTOS MADEMLIS (Senior Member, IEEE) was born in Greece, in February 1964. He received the Diploma degree (Hons.) in electrical engineering and the Ph.D. degree in electrical machines from the Aristotle University of Thessaloniki, Greece, in 1987 and 1997, respectively.

He was with the Electrical Machines Laboratory, Faculty of Electrical and Computer Engineering, Aristotle University of Thessaloniki, as a Research Associate, from 1990 to 2001; a Lecturer, from 2001 to 2006; an Assistant Professor, from 2007 to 2014; an Associate Professor, from 2014 to 2019; and has been a Professor, since 2019, where he has been the Director, since 2010. From 2013 to 2016, he was the Head of the Department of Electrical Energy. He was the Founder in 2013 and a Faculty Advisor with the Student Formula SAE Racing Team, Aristotle University of Thessaloniki, from 2013 to 2017. He is the author and coauthor of more than 100 peer-reviewed technical papers. His research interests include electrical machines and drives, especially in design and control optimization, renewable energy sources, electric vehicles, energy saving systems, and energy management in nearly zero energy buildings.

Dr. Mademlis was awarded the Fulbright Grant as a Visiting Professor from APED, Electrical and Computer Engineering Department, University of Connecticut, USA, in 2017.